Manuscript - Anggono et al. - JETS ID 14480 - 20201021_2

by Williyanto A

Submission date: 27-Oct-2020 11:05AM (UTC+0700)
Submission ID: 1427792212
File name: Manuscript_-_Anggono_et_al._-_JETS_ID_14480_-_20201021_2.pdf (3.61M)
Word count: 5087
Character count: 25073

Airflow Characteristics Investigation of a Diesel Engine for Different Helical Port Openings and Engine Speeds

Willyanto Anggono[1,2], Mitsuhisa Ichiyanagi[3], Reina Saito[3], Gabriel J. Gotama[2,4,5], Chris Cornelius[1,2], Ryera Kreshna[1,2], Takashi Suzuki[3]

[1]Mechanical Engineering Department, Petra Christian University, Surabaya, Indonesia
[2]Centre for Sustainable Energy Studies, Petra Christian University, Surabaya, Indonesia
[3]Department of Engineering and Applied Sciences, Sophia University, Tokyo, Japan
[4]School of Mechanical and Aerospace Engineering, Nanyang Technological University, Singapore
[5]Department of Aerospace and Geodesy, Technical University of Munich, Taufkirchen/Ottobrunn, Germany
Email: willy@petra.ac.id

Novelty: Previous studies of intake airflow characteristics were mostly performed in a two-valve engine and there is a stark difference between the airflow of two-valve and four-valve engines. Moreover, more studies are needed to understand the effect of helical port opening. Therefore, the intake airflow of a four-valve diesel engine with varying helical port openings was investigated.

Highlight:

- Variation of engine speeds and helical port openings do not cause a significant change in the location of the swirl center.
- Higher engine speed increases the turbulence intensity. However, it reduces the swirl ratio.
- Disruption of airflow with larger helical port opening reduces both the swirl ratio and the turbulence intensity.
- Trends of the swirl ratio and turbulence intensity are more evident when observed during the compression stroke.

Abstract. Intake airflow characteristics are essential to the performance of the diesel engine. However, previous investigations for the airflow characteristics were mostly performed in the two-valve engine despite the difference between the airflow of two-valve and four-valve engines. Therefore, in this study, particle image velocimetry investigations were performed in a four-valve diesel engine. The investigations were conducted under different engine speeds and helical port openings using a swirl control valve (SCV). The results suggest that the position of the swirl center does not significantly shift with different engine speeds and helical port opening as the dynamics of the flow remains closely similar. The trends for the airflow characteristics may be observed during the compression stroke. Higher engine speed increases the angular velocity of the engine more compared to the increase of the airflow velocity and resulted in a lower swirl ratio of the flow. On the other hand, higher engine speed brings higher mean velocity and the variation of the velocity that resulted in the larger turbulence intensity of the flow. Increasing the helical port opening brings a reduction in the swirl ratio

Received _____, Revised _____, Accepted for publication _____

and turbulence intensity as more airflow from the helical port disturbs the airflow from the tangential port.

Keywords: *airflow; particle image velocimetry; swirl control valve; swirl ratio; turbulence intensity*

1 Introduction

Diesel engines are the most commercially used land-based vehicles due to their higher thermal efficiency in comparison with gasoline engines [1]. Over the recent years, the increased demand for energy due to the rise in the population [2], the overreliance in fossil fuels [3], and the need to decrease the negative emissions [4-6] have put more stringent regulations in the design of engines. Several methods have been devised to improve the emissions of diesel engines which include the use of biofuel [7,8], manipulating the intake air mass and temperature [9], as well as generating swirl and tumble motion in the airflow.

In a diesel engine, swirl flow may be generated using a helical intake port and it is considered to be more essential than the tumble motion [10]. Swirl flow promotes turbulence characteristics in the airflow for better mixing of the fuel-air mixture through the disintegration of the molecule of the fuel [11,12]. Swirl flow reduces ignition delay in the combustion process that leads to reduced soot and NOx emissions [13,14] despite simultaneous Soot and NOx emissions reductions are usually considered difficult to achieve as there is a trade-off between them [1]. Swirl flow was also found to reduce the burning duration, increase flame speed, extend the flammability limit, increase the thermodynamic heat transfer, and improve the thermal efficiency in a combustion process [15,16].

Several studies have been performed to understand the parameters that affect the swirl and turbulence characteristics of the airflow in the combustion chamber. Dawat and Venkitachalam [17] conducted a numerical investigation of swirl flow generated by various geometries and orientations of a helical port in a four-valve

engine. The study suggested that the design and orientation of the helical port affect the swirl ratio and the turbulent kinetic energy. They also found that under similar helical intake port design, faster engine speed decreases the swirl ratio and larger variation of swirl ratio is found at higher engine speed. Catania and Spessa [18] conducted a study using a helicoidal intake port to generate a counterclockwise swirl flow in a two-valve high-squish engine under differing engine speeds of 600 to 3000 RPM. They concluded that, for a two-valve engine, an intense high-frequency turbulence production occurs in the intake stroke and starts to decay at the end of intake stroke/start of the compression stroke. They also suggested that the trend for mean velocity, turbulence intensity, and mean-velocity fluctuation that scale with the engine speed can be observed during most of the compression stage.

Other than the engine speed, the SCV (swirl control valve) also plays a role in the quality of the intake airflow. Kim et al. [19] investigated the effect of SCV in the tangential port to the flow characteristics at a distance 37 mm away from the engine head of a four-valve diesel engine. They found an increase in the swirl ratio by applying SCV closing in the tangential port. However, they also found that the mass flow rate decreases with SCV closing due to the reduced area of the intake port. Matsushita et al. [20] applied SCV in a helical port of SI engine and found an increase in the combustion performance due to the high swirl ratio in closed SCV at partial load. Under full load condition, SCV allows the engine to consistently have high performance.

While the generation of swirl and turbulence flows in combustion cylinders have been studied extensively, the effect of swirl flow generated by helical intake port in four-valve diesel engines has not received much attention [17]. Kim et al. [19] have suggested that the airflow characteristics between two-valve and four-valve engines are exceptionally contrasting, indicating the necessity to investigate the

airflow of a four-valve engine. Furthermore, the effect of various SCV openings on the helical intake port paired with a fully opened tangential intake port has not been comprehensively investigated as well. Therefore, in this study, the swirl ratio and the turbulence intensity in the combustion chamber of a four-valve diesel engine were investigated using PIV (Particle Image Velocimetry) technique under various engine speeds and opening of the helical intake port.

2 Methods

The experiment was conducted using an optical four strokes single-cylinder diesel engine with four valves. The bore and the length stroke of the engine are 85 mm and 96.9 mm, respectively. The cavity diameter of the chamber is 51.6 mm and the engine has a compression ratio of 16.3. One helical and one tangential intake ports were used in this study as this combination generates a higher swirl ratio compared to two tangential or two helical ports [21]. The location of the ports as seen from the top of the cylinder, and the coordinate axes in the x, y and z directions are shown in Figure 1. Laser Nd:YAG double-pulse 532-nm (Continuum, Mesa-PIV) with pulse generator (FLOWTECH RESEARCH, VSD2000) was used to generate a laser sheet. The laser sheet has a thickness of 1 mm and was irradiated perpendicularly to the center axis of the cylinder and positioned 60 mm from the top of the cylinder to develop a two-dimensional plane (z = 60 mm). Particle images from the reflection of the mirror were taken from the bottom of the engine with a high-speed camera (Photron, FASTCAM SA5) at a resolution of 696 x 704 pixels and a time resolution of 15 kHz. One pair image per two °CA (Crank Angle) was taken in an interval of 20 μs. Tracer Silica particles (SiO_2) with an average particle size of 4.65 μm were mixed into the intake air using generator seeding (PIVTECH GmbH) and air compressor (EARTH MAN, ACP-25SLA).

Particle images were analyzed using PIV (Flowtech Research FtrPIV) analysis software with a direct cross-correlation algorithm [22]. The inspection area was set to 16 pixels and the search area was set to 33 pixels. The setup has been used by the author in a previous study [23] and other research group has used a similar setup to investigate the airflow characteristics in a combustion cylinder [24]. The photograph and the schematic of the experimental setup are provided in Figure 2.

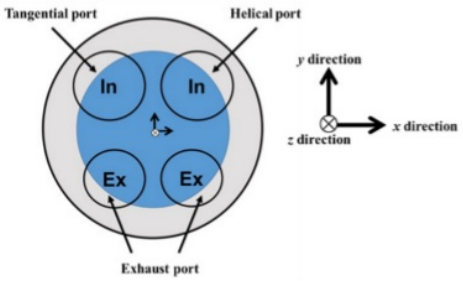

Figure 1 Ports location as seen from the top of the combustion cylinder.

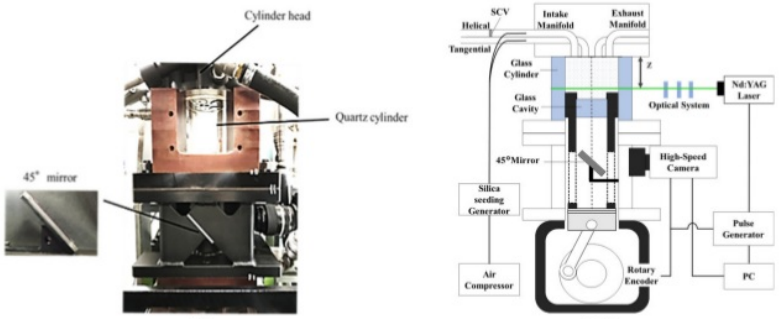

Figure 2 (a) Photograph of the experimental setup and (b) schematic of the experimental setup.

In this study, two sets of experiments were performed. The first set was conducted under various engine speeds for fully opened tangential and helical ports, which corresponds to 100% SCV opening. The second experiment was conducted under constant engine speed with the various opening of the helical port to modify the

SCV opening. This is in contrast with the study by Kim et al. [19] where the SCV was applied in the tangential port instead. For this study, the percentage of SCV opening was defined by the velocity of the flow that passes through the ports. Summary of the experimental conditions for the first and second sets of experiments are given in Tables 1 and 2, respectively.

Table 1 Parameters for the first set of experiments.

Tangential Port Opening	Helical Port Opening	SCV Opening	Engine Speed
100%	100%	100%	1000 RPM
100%	100%	100%	1200 RPM
100%	100%	100%	1500 RPM

Table 2 Parameters for the second set of experiments.

Tangential Port Opening	Helical Port Opening	SCV Opening	Engine Speed
100%	25% (1/4 Helical)	25%	1000 RPM
100%	50% (1/2 Helical)	50%	1000 RPM
100%	75% (3/4 Helical)	75%	1000 RPM
100%	100%	100%	1000 RPM

For both sets of experiments, the engine was operated under naturally aspirated condition. The Stokes number was set to 0.00354, 0.00425, 0.00531, for an engine speed of 1000 RPM, 1200 RPM, 1500 RPM, respectively. The number of cycles measured is 32 consecutive cycles for all conditions with 0 °CA is defined as the TDC of the intake stroke. The experiment was performed for two replications and the average of the results was taken as the mean velocity. The measured mean velocity was used to calculate the swirl ratio and turbulence intensity. The swirl ratio is defined as the normalized average angular velocity of the rotating flow in the measured plane, as mathematically described in Eq. 1. The turbulence intensity is defined as the resultant of the standard deviation of the velocity, as mathematically described in Eq. 2. More emphasis on the results are put in crank angles of 110, 180, and 250 °CA which correspond to condition

during the intake stroke, the end of the intake stroke/start of the compression stroke, and during the compression stroke, respectively.

$$S_R = \frac{1}{\omega_{engine}} \frac{1}{N} \sum_{l=1}^{N} \left[\frac{v_{i,j} \cos\theta - u_{i,j} \sin\theta}{r_{i,j}} \right]_l \quad (1)$$

Where S_R is the swirl ratio, ω_{engine} is the angular velocity of the engine, N is the total number of discretized points of the plane, θ and $r_{i,j}$ are the angle and cartesian coordinate of a point, respectively, while $u_{i,j}$ and $v_{i,j}$ are the velocity in the horizontal and vertical directions, respectively.

$$T_I = \frac{1}{N} \sum_{l=1}^{N} \sqrt{[(U_{rms})^2 + (V_{rms})^2]_l} \quad (2)$$

Where T_I is the turbulence intensity, U_{RMS} is the root-mean-square of the velocity in the x-direction, and V_{RMS} is the root-mean-square of the velocity in the y-direction.

3 Results and Discussion

3.1 Swirl Ratio and Turbulence Intensity Under Various Engine Speeds (First Set of Experiment)

Figure 3 shows the mean velocity profile for various engine speeds at different crank angles. In this figure, the swirl center can be identified as the epicenter of the vectors and have very low mean velocity. At 110 °CA, the swirl center resides near the tangential port (upper left) for all engine speeds experimented. For 180 °CA, the swirl center resides near the left exhaust port (lower left) for all engine speeds investigated. For 250 °CA, the swirl center is in the vicinity of the right exhaust port (bottom right) for all engine speeds investigated. These results suggest that the increase in engine speed does not cause a dramatic change in the swirl center. This is because the higher engine speed leads to a similarly larger proportion of mass flow and mean velocity of the flow for both intake ports, and therefore does not significantly alter the dynamic of the flow within the chamber.

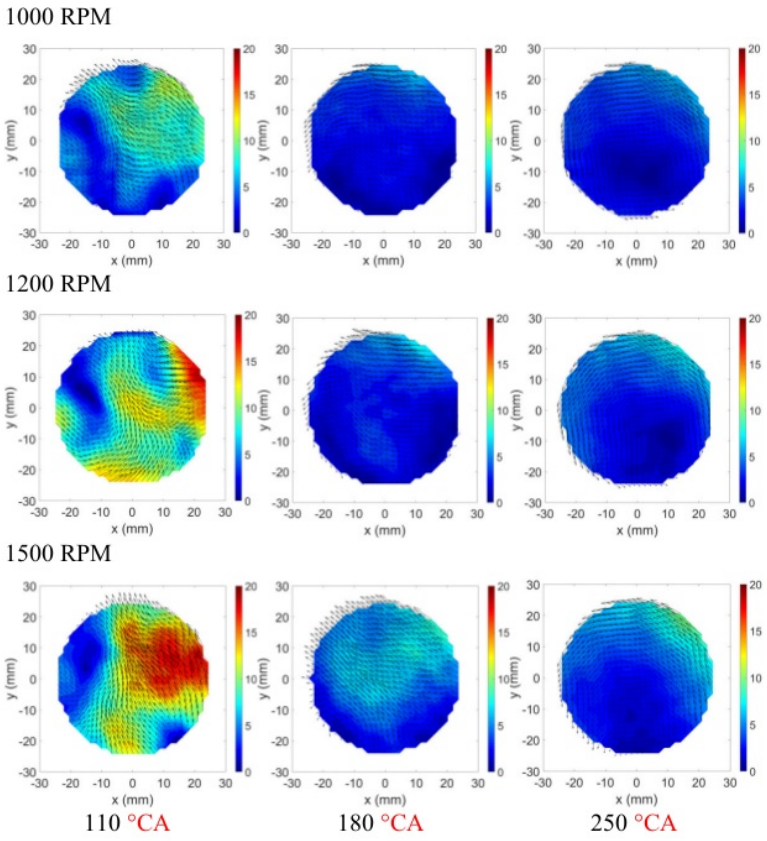

Figure 3 Mean velocity profile (in m/s) of the airflow under various engine speeds for 110, 180, and 250 °CA.

Figure 4 shows the turbulence intensity profile of the cylinder under various engine speeds and crank angles. Unlike the swirl center, it is difficult to pinpoint the maximum turbulence intensity from the figures; therefore, the coordinates for the largest turbulence intensity under various engine speeds and crank angles are given in Table 3. The overall trend indicates that the turbulence intensity reduces with lower engine speed and higher crank angles. The location for the maximum

195 turbulence intensity varies between engine speeds and crank angles with no clear
196 trend. However, it is observed that for all the conditions except 1000 RPM and
197 250 °CA, the location of the highest turbulence intensity tends to be on the right
198 side near the vicinity of helical or right exhaust ports. This is expected as the
199 helical port generates swirl flow in its vicinity that lead to a large variation of
200 velocity and therefore large turbulence intensity.

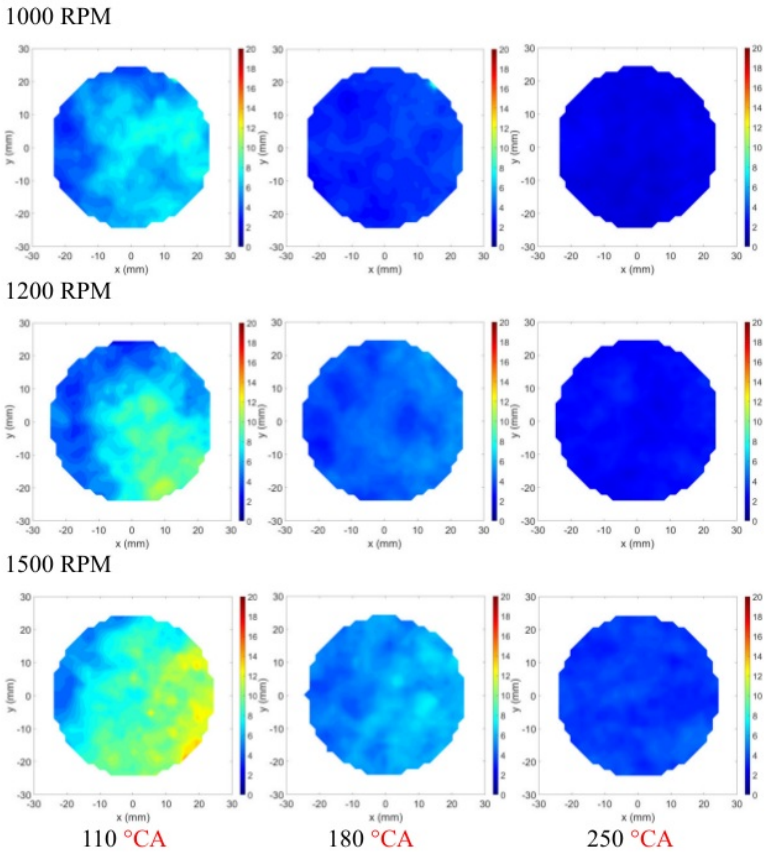

201

202 **Figure 4** Turbulence intensity profile (in m/s) of the airflow under various engine
203 speeds for 110, 180, and 250 °CA

Table 3 Coordinates of the maximum turbulence intensity (in mm) under various engine speeds for 110, 180, and 250 °CA.

Parameters	110 °CA	180 °CA	250 °CA
1000 RPM	x = 13.2 y = 21.0	x = 14.9 y = 19.3	x = -23.4 y = 1.8
1200 RPM	x = 9.9 y = -18.7	x = 13.3 y = 19.3	x = 20.2 y = 12.4
1500 RPM	x = 15.8 y = -19.0	x = 13.3 y = -1.5	x = 21.0 y = -12.1

To further analyze the results, the swirl ratio and the turbulence intensity were plotted for the entirety of the crank angle observed. Figure 5(a) shows the swirl ratio as a function of the crank angle for various engine speeds. Near 110 °CA (during the intake stroke), the swirl ratio reached its peak and afterwards dramatically decreases with the increase of crank angle to near 180 °CA (end of intake stroke/start of compression stroke). At near 180 °CA, the swirl ratio starts to increase up to 250 °CA (during the compression stroke). An exception was found in the 1000 RPM where the dip of the swirl ratio occurred earlier (~140 °CA) and therefore the increase of the swirl ratio also starts earlier (~150 °CA). The clear trend of the swirl ratio can be observed at the compression stroke (180 to 250 °CA) with the swirl ratio tends to be inversely proportional to the engine speed. The reason behind this can be traced in the mathematical definition of swirl ratio in Eq. 1. While the velocity of the flow, which is proportional to the swirl ratio, increases with engine speed, the angular velocity of the engine, which is inversely proportional to the swirl ratio, also increases. However, when the velocity of the flow increases, the airflow interferes with the cylinder and the friction increases. From the above, the increase of the velocity of the flow is less than the increase of the angular velocity of the engine and therefore higher engine speed reduces the swirl ratio.

Figure 5(b) shows the turbulence intensity as a function of the crank angle under various engine speeds. There is a clear trend of the turbulence intensity

throughout the observed crank angle. The flow tends to be highly turbulence during the intake stroke and decreases as it goes towards the compression stroke. The results also suggested that the turbulence intensity is proportional to the engine speed as higher engine speed leads to a higher mean velocity that instigates the variation of the velocity and the turbulence behavior of the airflow.

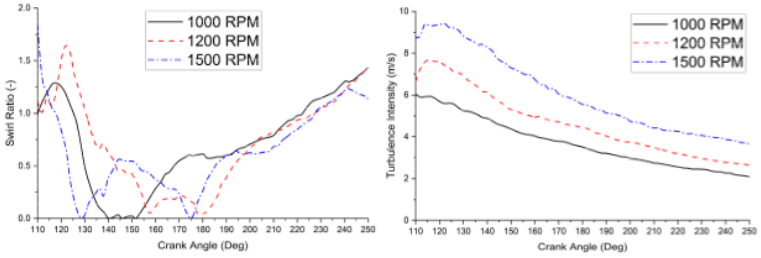

(a) (b)

Figure 5 (a) Swirl ratio and (b) turbulence intensity of the airflow as a function of crank angle under various engine speeds.

3.2 Swirl Ratio and Turbulence Intensity Under Various SCV Openings (Second Set of Experiment)

Figure 6 shows the mean velocity for various helical port openings (percentage of SCV) and crank angles. For 110 °CA, the swirl center is located near the tangential intake port (upper left) and the variation of SCV openings does not cause a significant shift in the location of the swirl center. Similarly, for 180 and 250 °CA, the SCV openings do not vary the location of the swirl center that is located in the vicinity of the left exhaust port (lower left) and right exhaust port (lower right), respectively. While smaller SCV opening reduces the intake flow area of the helical port, it merely leads to lower mass flow rate and higher mean velocity of the flow without significantly altering the dynamics of the flow inside the chamber.

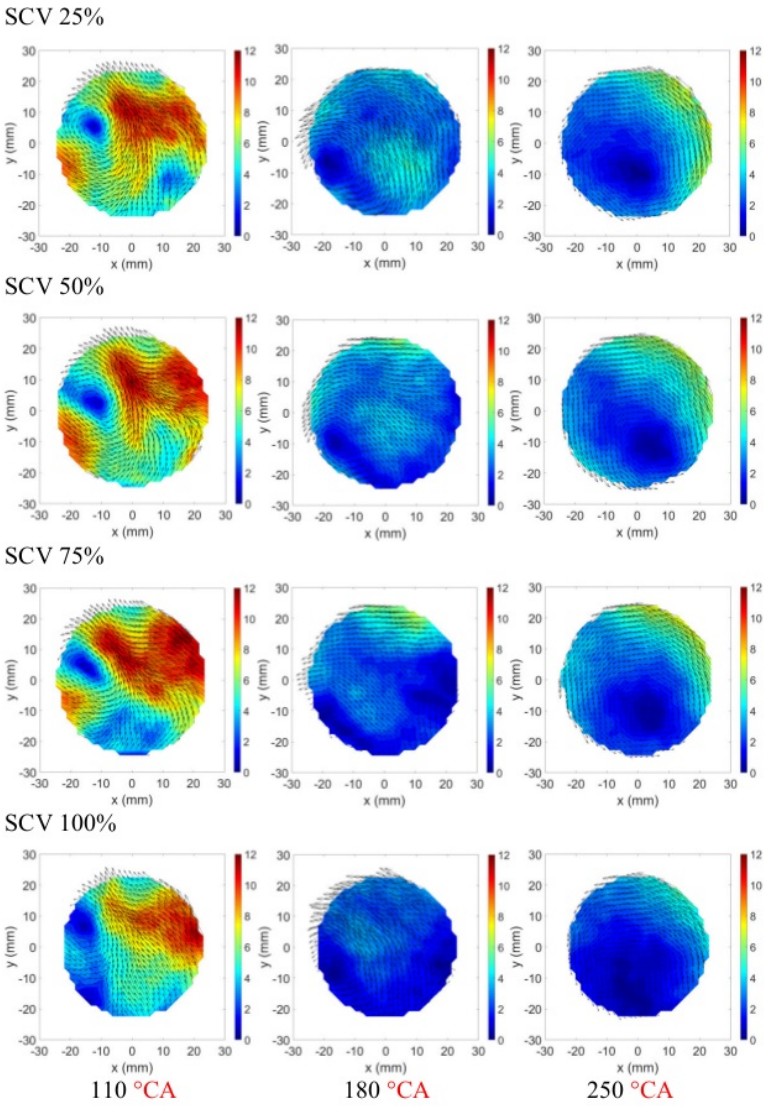

Figure 6 Mean velocity profile (in m/s) of the airflow under various SCV openings for 110, 180, and 250 °CA.

As for the turbulence intensity, Figure 7 shows the distribution of turbulence intensity for various helical port openings (SCV openings) and crank angles with Table 4 showing the coordinates for the maximum turbulence intensity. It can be inferred that there is a clear trend of lower turbulence intensity with a larger crank angle. However, in terms of location for the maximum turbulence intensity, the effect of SCV openings does not have a clear trend. Similar to the first set of experiments, the majority of the maximum turbulence intensity is located on the right side; either near the helical port or the right exhaust port due to the swirl flow generated by the helical port.

By observing the swirl ratio for all crank angles studied, as shown in Figure 8(a), it was found that the swirl ratio is at its peak during the intake stroke and gradually decreases with higher crank angle up to a certain angle. Near the start of the compression stroke (~160 to 180 °CA), the swirl ratio increases until 250 °CA. Similar to the first set of experiments, the trend of swirl ratio to crank angles for different SCV openings is observed during the compression stroke. The swirl ratio decreases with larger SCV opening as more mass flow originated from the helical port disrupted the airflow coming from the tangential port, reducing the velocity of the flow inside the chamber.

Figure 8(b) shows the turbulence intensity of the airflow for all crank angles studied. The turbulence intensity shows a clear trend and the difference between SCV openings with higher SCV opening leads to lower turbulence intensity. This is due to the larger helical port opening that disrupts the airflow from the tangential port and reduces the variation of the velocity and turbulence behavior in the airflow of the chamber.

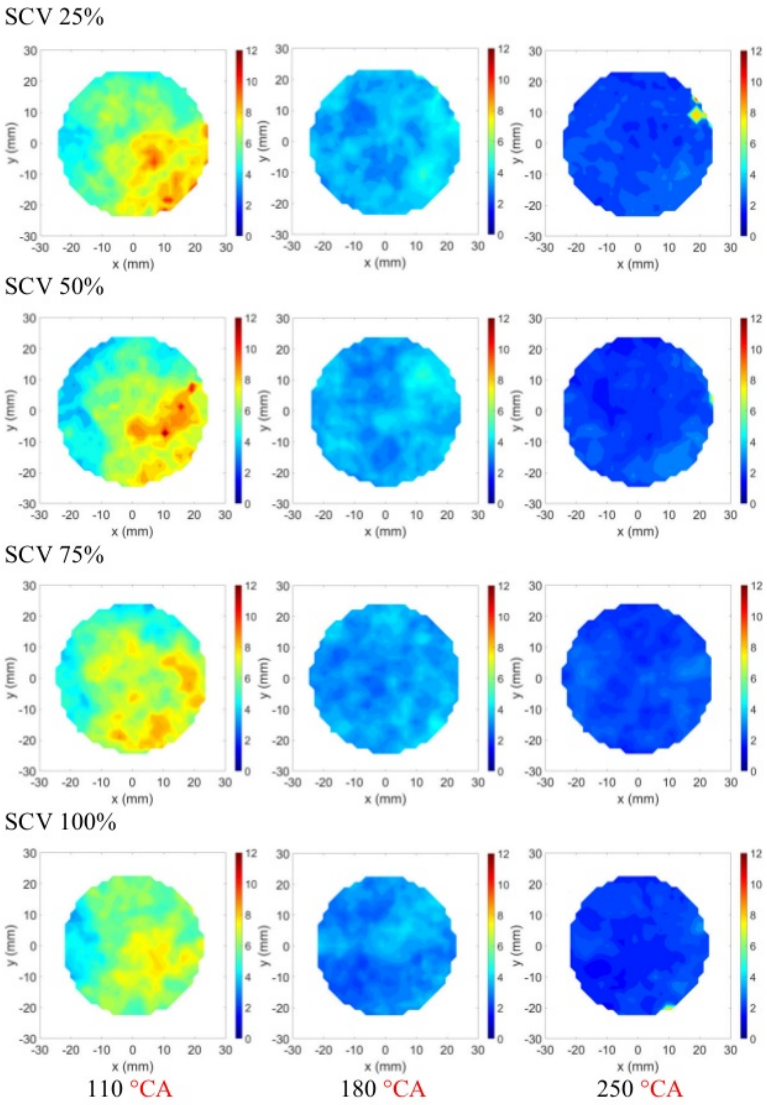

Figure 7 Turbulence intensity profile (in m/s) of the airflow under various SCV openings for 110, 180, and 250 °CA

Table 4 Coordinates of the maximum turbulence intensity (in mm) under various SCV openings for 110, 180, and 250 °CA.

Parameters	110 °CA	180 °CA	250 °CA
SCV 25%	x = 10.3 y = -21.9	x = 17.2 y = 17.9	x = 18.9 y = 14.4
SCV 50%	x = 10.6 y = -7.3	x = 10.6 y = 11.7	x = 24.4 y = 4.8
SCV 75%	x = -4.0 y = -19.3	x = 18.4 y = -15.8	x = 15.0 y = 1.5
SCV 100%	x = 7.5 y = -5.1	x = 17.8 y = 13.9	x = 9.2 y = -20.7

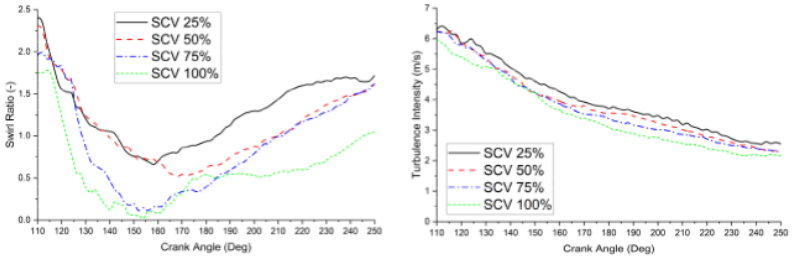

(a) (b)

Figure 8 (a) Swirl ratio and (b) turbulence intensity of the airflow as a function of crank angles under various SCV openings

4 Conclusion

The airflow characteristics of the four-valve single-cylinder engine have been investigated using the PIV technique for various engine speeds and SCV (helical intake port) openings. The results suggested that the engine speed and SCV opening do not have a significant influence on the location of the swirl center as the dynamics of the flow inside the chamber remains closely similar. However, higher engine speed leads to lower swirl ratio as the angular velocity of the engine increases more in comparison with the velocity of the flow due to the friction between the flow and cylinder. On the other hand, higher engine speed brings higher turbulence intensity due to the increased mean velocity and the variation of the velocity in the flow. As for SCV opening, higher SCV opening leads to the reduction of both swirl ratio and turbulence intensity due to the increased mass

flow from the helical intake port. It disrupts the airflow coming from the tangential port and reduces the mean velocity as well as the variation of the velocity in the flow. Those trends that were found in the present study are more easily observed during the compression stroke.

Acknowledgment

This research was supported by the Japan Society for the Promotion of Science, Grants-in-Aid for Scientific Research (No. 19K04244), Sophia University Special Grant for Academic Research, Research in Priority Areas, and Petra Christian University under project code: 451/FTI/UKP/2019. The authors would like to express their gratitude towards both Sophia University, Japan, and Petra Christian University, Indonesia, for the supports in this study.

Nomenclature

N	=	Total number of discretized points [-]
$r_{i,j}$	=	Cartesian coordinate of a point [m]
S_R	=	Swirl ratio [-]
T_I	=	Turbulence intensity [m/s]
θ	=	The angle of a discretized point [rad]
U_{RMS}	=	Root mean square of the velocity in x-direction [m/s]
$u_{i,j}$	=	Velocity in horizontal direction [m/s]
V_{RMS}	=	Root mean square of the velocity in y-direction [m/s]
$v_{i,j}$	=	Velocity in vertical direction [m/s]
ω_{engine}	=	Angular velocity of the engine [rad/s]

References

[1] Anggono, W., Ikoma, W., Chen, H., Liu, Z., Ichiyanagi, M., Suzuki, T. & Gotama, G.J., *Investigation of Intake Pressure and Fuel Injection Timing Effect on Performance Characteristics of Diesel Engine*, IOP Conference Series: Earth and Environmental Science, **257**(1), 012037, May 2019.

[2] Jazie, A.A, *DBSA-catalyzed Sewage Sludge Conversion into Biodiesel in a CSTR: RSM optimization and RTD Study*, Journal of Engineering and Technological Sciences, **51**(4), pp. 537–555, Aug. 2019.

[3] Mahidin, Gani, A., Muslim, A., Husin, H., Hani, M.R., Syukur, M., Hamdani, Khairil & Rizal, S., *Sulfur Removal in Bio-Briquette Combustion Using Seashell Waste Adsorbent at Low Temperature*, Journal of Engineering and Technological Sciences, **48**(4), pp. 465–481, Sept. 2016.

[4] Dewi, K., Khair, H. & Irsyad, M., *Development of Green Pavement for Reducing Oxides of Nitrogen (NOx) in the Ambient Air*, Journal of Engineering and Technological Sciences, **48**(2), pp. 159–172, May 2016.

[5] Kodancha, P., Pai, A., Kini, C.R. & Bayar, R.K., *Performance Evaluation of Homogeneous Charge Compression Ignition Combustion Engine – A Review*, Journal of Engineering and Technological Sciences, **52**(3), pp. 289–309, May 2020.

[6] Thonglek, V. & Kiatsiriroat, T., *Use of Pulse-Energized Electrostatic Precipitator to Remove Submicron Particulate Matter in Exhaust Gas*, Journal of Engineering and Technological Sciences, **46**(3), pp. 271–285, Apr. 2014.

[7] Anggono, W., Noor, M.M., Suprianto, F.D., Lesmana, L.A., Gotama, G.J. & Setiyawan, A., *Effect of Cerbera Manghas Biodiesel on Diesel Engine Performance*, International Journal of Automotive and Mechanical Engineering, **15**(3), pp. 5667–5682, Sept. 2018.

[8] Anggono, W., Hayakawa, A., Okafor, E.C., Gotama, G.J. & Wongso, S., *Laminar Burning Velocity and Markstein Length of CH_4/CO_2/Air Premixed Flames at Various Equivalence Ratios and CO_2 Concentrations Under Elevated Pressure*, Combustion Science and Technology, in-press, Mar. 2020. https://doi.org/10.1080/00102202.2020.1737032

[9] Yilmaz, E., Ichiyanagi, M. & Suzuki, T., *Development of Heat Transfer Model at Intake System of IC Engine with Consideration of Backflow Gas Effect*, International Journal of Automotive Technology, **20**(5), pp. 1065–1071, Oct. 2019.

[10] Zha, K., Busch, S., Miles, P.C., Wijeyakulasuriya, S., Mitra, S. & Senecal, P.K., *Characterization of Flow Asymmetry During the Compression Stroke Using Swirl-Plane PIV in a Light-Duty Optical Diesel Engine with the Re-entrant Piston Bowl Geometry*, SAE International Journal of Engines, **8**(4), 2015-01-1699, Apr. 2015.

[11] Agarwal, A.K., Gadekar, S. & Singh, A.P., *In-cylinder Air-flow Characteristics of Different Intake Port Geometries Using Tomographic PIV*, Physics of Fluids, **29**(9), 095104, Sep. 2017

[12] Perini, F., Miles, P.C. & Reitz, R.D., *A Comprehensive Modeling Study of In-cylinder Fluid Flows in a High-swirl, Light-duty Optical Diesel Engine*, Computers and Fluids, **105**, pp. 113–124, Sep. 2014.

[13] Lakshminarayanan, P.A. & Kumar, A., *Design and Development of Heavy Duty Diesel Engines*, ed. 1, Springer. 2020.

[14] Raj, R.T.K. & Manimaran, R., *Effect of Swirl in a Constant Speed DI Diesel Engine Using Computational Fluid Dynamics*, CFD Letters, **4**(4), pp. 214–224, Dec. 2012.

[15] Hill, P.G. & Zhang, D., *The Effects of Swirl and Tumble on Combustion in Spark-Ignition Engines*, Progress in Energy and Combustion Science, **20**(5), pp. 373–429, June 1994.

[16] Varun, Singh, P., Tiwari, S.K., Singh, R. & Kumar, N., *Modification in Combustion Chamber Geometry of CI engines for Suitability of Biodiesel: A review*, Renewable and Sustainable Energy Reviews, **79**, pp. 1016–1033, May 2017.

[17] Dawat, V.K., & Venkitachalam, G., *Influence of a High-Swirling Helical Port with Axisymmetric Piston Bowls on In-Cylinder Flow in a Small Diesel Engine*, SAE Technical Papers, **2016-01-0587**, Apr. 2016.

[18] Catania, A.E. & Spessa, E., *Speed Dependence of Turbulence Properties in a High-squish Automotive Engine Combustion System*, SAE Technical Paper, **105**, pp. 313–334, 1996.

[19] Kim, Y., Han, Y. & Lee, K.A., *Study on The Effects of The Intake Port Configurations on The Swirl Flow Generated in A Small D.I. Diesel Engine*, Journal of Thermal Science, **23**(3), pp. 297–306, May 2014

[20] Matsushita, S., Inoue, T., Nakanishi, K., Okumura, T. & Isogai, K., *Effects of Helical Port with Swirl Control Valve on The Combustion and Performance of S.I. Engine*, SAE Technical Papers, **94**(850046), pp. 17–22, Feb. 1985.

[21] Jia, D.W., Deng, X.W. & Lei, J.L., *Steady-State Experiment and Simulation of Intake Ports in A Four-Valve Direct Injection Diesel Engine*, Journal of Applied Fluid Mechanics, **11**(1), pp. 217–224, 2018.

[22] Raffel, M., Willert, C.E., Wereley, S.T. & Kompenhans, J., *Particle Image Velocimetry*, ed. 1, Springer-Verlag, 2007.

[23] Ichiyanagi, M., Ndizeye, G., Sawamura, Y., Saito, R., Takahashi, K., Otsubo, K., Chen, H. & Takashi, S., *Improvement of On-board In-cylinder Gas Flow Model and Wall Heat Transfer Prediction Model for CI Engines Using CFD Analysis and PIV Measurements under Motoring and Firing Conditions*, SAE Technical Paper, **2019-32-0542**, Jan. 2020.

[24] Petersen, B. & Miles, P., *PIV Measurements in the Swirl-Plane of a Motored Light-Duty Diesel Engine*, SAE International Journal of Engines, **4**(1), pp. 1623–1641, Apr. 2011.

Manuscript - Anggono et al. - JETS ID 14480 - 20201021_2

ORIGINALITY REPORT

2%	1%	1%	0%
SIMILARITY INDEX	INTERNET SOURCES	PUBLICATIONS	STUDENT PAPERS

PRIMARY SOURCES

1	www.tandfonline.com Internet Source	1%
2	"Rough Sets and Current Trends in Computing", Springer Science and Business Media LLC, 2010 Publication	1%

Exclude quotes	On	Exclude matches	< 30 words
Exclude bibliography	On		